

# Performance Analysis of Solid-oxide Electrolysis Cells for Syngas Production by H<sub>2</sub>O/CO<sub>2</sub> Co-electrolysis

Dang Saebea<sup>a</sup>, Suthida Authayanun<sup>b</sup>, Yaneeporn Patcharavorachot<sup>c</sup>, Soipatta Soisuwan<sup>a</sup>, Suttichai Assabumrungrat<sup>d</sup>, Amornchai Arpornwichanop<sup>e</sup>

<sup>a</sup>Department of Chemical Engineering, Faculty of Engineering, Burapha University, Chonburi 20131, Thailand

<sup>b</sup>Department of Chemical Engineering, Faculty of Engineering, Srinakharinwirot University, Nakorn Nayok 26120, Thailand

<sup>c</sup>School of Chemical Engineering, Faculty of Engineering, King Mongkut's Institute of Technology Ladkrabang, Bangkok 10520, Thailand

<sup>d</sup>Center of Excellence on Catalysis and Catalytic Reaction Engineering, Department of Chemical Engineering, Chulalongkorn University, Bangkok 10330, Thailand

<sup>e</sup>Computational Process Engineering Research Unit, Department of Chemical Engineering, Faculty of Engineering, Chulalongkorn University, Bangkok 10330, Thailand  
[dangs@eng.buu.ac.th](mailto:dangs@eng.buu.ac.th)

High-temperature solid oxide electrolysis cells (SOECs) are promising technologies to store excess renewable energy generation. In this work, the mathematical model of SOEC, which can describe the behaviour of a cathode-supported SOEC operating for H<sub>2</sub>O and CO<sub>2</sub> co-electrolysis, is developed from mass balance, dusty gas model, and electrochemical model. The validated SOEC model is used to analyse the influence of the reversible water-gas shift reaction taking place on the cathode on the performance of the SOEC for syngas production. The simulation results show that the reverse water-gas shift reaction is highly pronounced at the cathode surface due to high CO<sub>2</sub> component and can contribute to CO production. The rate of water-gas shift reaction increases along the depth of the cathode to the three-phase boundary. At the three-phase boundary, an increase in operating temperatures results in the enhancement of the rate of water-gas shift reaction. Additionally, regarding the SOEC performance, the electrical energy consumed for co-electrolysis in SOEC decreases with increasing temperature because the activation overpotentials and ohmic overpotentials are lower.

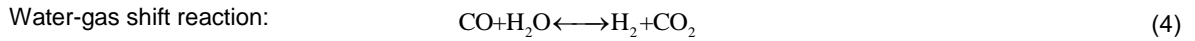
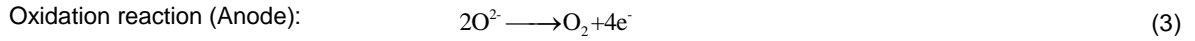
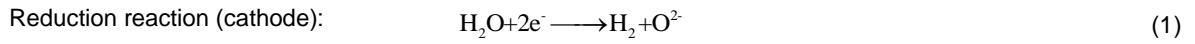
## 1. Introduction

The global energy consumption has increased continuously whereas fossil fuel as main energy has depleted. Presently, renewable energy sources, such as solar and wind, have received considerable attention due to their abundance and sustainability (Saebea et al., 2016). However, these types of energy are restricted in time and space, intermittence, and site specific. Hydrogen production technologies have been developed rapidly (Saebea et al., 2014). The use of electricity from solar cells or wind turbines to produce hydrogen via electrolyzers is a promising way to convert their unstable energies to a stable chemical energy (Ebbesen et al., 2012). Among various types of the electrolysis cells, solid oxide electrolysis cells (SOECs) have received considerable attention because of their high efficiency and high feed impurity tolerance (Ferrero et al., 2013). Additionally, the SOECs are able to reduce an amount of CO<sub>2</sub> by electrolysis of CO<sub>2</sub> to CO. In general, the CO<sub>2</sub> electrolysis consumes high electrical power (Kazempoor & Braun, 2015). However, the power consumption of CO<sub>2</sub> electrolysis can be reduced by simultaneously electrolyzing H<sub>2</sub>O and CO<sub>2</sub> because more CO can be generated via the reverse water-gas shift (RWGS) reaction (Menon et al., 2014). Because the RWGS reaction is reversible, the reaction direction depends on its operating conditions. As the electrochemical reactions, kinetic reactions, mass transfers, and charge transfers of H<sub>2</sub>O/CO<sub>2</sub> co-electrolysis in SOEC are quite complicated. The understanding of primary operating parameters on physical phenomenon in SOEC is required to provide its optimal conditions.

The aim of this study is to analyse the influence of the RWGS reaction taking place on the cathode and the SOEC performance for the syngas production. The SOEC model is based on mass balances, the electrochemical model, and the dusty gas model to explain the multiple reactions and multi-component mass transport in SOEC. Additionally, the influence of operating temperatures on the cell performance is investigated.

## 2. Modelling of SOEC

A planar solid oxide electrolysis cell (SOEC) is considered in this study, as shown in Figure 1. The production of H<sub>2</sub> and CO in SOEC needs the electricity input in order to proceed the electrolysis reaction. H<sub>2</sub>O and CO<sub>2</sub> are converted to H<sub>2</sub> and CO at the cathode/electrolyte interface via co-electrolysis (Eqs (1) and (2)). Oxygen ions produced at the cathode diffuse through the electrolyte to the anode and the oxygen occurs from the oxidation reaction at the anode, shown in Eq(3). Moreover, the WGS reaction occurs at the cathode porous material of SOEC and can be expressed in Eq(4). The WGS reaction as the equilibrium reaction over nickel catalyst can shift forward and backward reactions depending on the operating condition. This reaction has an important influence on the CO production and can reduce the power input in the SOEC (Ni, 2012).



The gaseous species in air and fuel channels transport in the electrode to the three-phase boundary. The RWGS reaction takes place in the porous cathode. The transports of gas molecules in the electrode are considered as the one-dimensional diffusion along the electrode thickness from the reaction-diffusion equation, which is given by:

$$\frac{\varepsilon}{RT} \frac{\partial(y_i P)}{\partial t} = -\nabla N_i + R_i \quad (5)$$

where  $y_i$  is the molar fraction of component  $i$ ,  $\varepsilon$  is the electrode porosity,  $P$  is the total pressure,  $R_i$  is the reaction rate of component  $i$ , and  $N_i$  is the molar flux of component  $i$ .

The molar flux of multi-component H<sub>2</sub>-H<sub>2</sub>O-CO-CO<sub>2</sub> systems is represented by the dusty gas model, which can express the relationship between molar fluxes, molar concentrations, pressure gradient, and concentration gradients as:

$$\frac{N_i}{D_{i,k}^{eff}} + \sum_{j=1, j \neq i}^n \frac{y_j N_j - y_i N_j}{D_{ij}^{eff}} = -\frac{P}{RT} \frac{dy_i}{dx} \quad (6)$$

where  $D_{i,k}^{eff}$  is the Knudsen diffusivity of component  $i$  and  $D_{ij}^{eff}$  is the binary diffusivity of component between  $i$  and  $j$ .

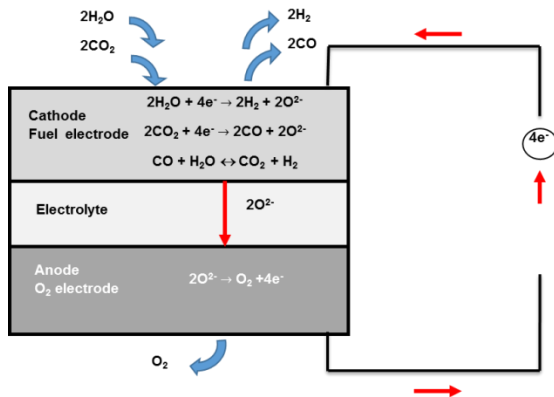


Figure 1: Schematic side view of a planar solid oxide electrolysis cell.

The net current density is the sum of current density for the H<sub>2</sub>O electrolysis and CO<sub>2</sub> electrolysis. The partition ratio of the current density of H<sub>2</sub>O and CO<sub>2</sub> at the electrode/electrolyte interface is calculated from the normalization factor ( $\gamma$ ), which is given by

$$i = I_{H_2} + I_{CO} = \gamma i_{H_2} + (1-\gamma) i_{CO} \quad (7)$$

where

$$\gamma = \frac{y_{H_2O}^{TPB}}{y_{H_2O}^{TPB} + y_{CO_2}^{TPB}} \quad (8)$$

The difference of thermodynamic potential among the electrode reactions is the reversible potential that can be calculated by the Nernst equation as:

$$E_{H_2}^{rev} = E_{H_2}^0 + \frac{RT}{2F} \ln \left[ \frac{P_{H_2}^{TPB} (P_{O_2}^{TPB})^{\frac{1}{2}}}{P_{H_2O}^{TPB}} \right] \quad (9)$$

$$E_{CO}^{rev} = E_{CO}^0 + \frac{RT}{2F} \ln \left[ \frac{P_{CO}^{TPB} (P_{O_2}^{TPB})^{\frac{1}{2}}}{P_{CO_2}^{TPB}} \right] \quad (10)$$

where  $E^0$  the open-circuit potential at standard pressure and  $P_i^{TPB}$  is the partial pressure of component  $i$ .

The cell performance can be evaluated from the cell operating voltage (Eqs (11) and (12)). The actual cell voltage,  $V_{cell}$ , is more than the reversible voltage. This is due to the overpotential and internal resistance losses, i.e., the ohmic overpotential ( $\eta_{ohm}$ ) and the activation overpotentials ( $\eta_{act}$ ).

$$V_{cell} = E_{H_2}^{rev} + |\eta_{ohm}(i_{H_2})| + |\eta_{act}(i_{H_2})| \quad (11)$$

$$V_{cell} = E_{CO}^{rev} + |\eta_{ohm}(i_{CO})| + |\eta_{act}(i_{CO})| \quad (12)$$

The ohmic overpotential can be expressed as:

$$\eta_{ohm} = iR_T \quad (13)$$

where  $R_T$  is the internal resistance of cell related to the thickness and the conductivity as:

$$R_T = \frac{d_e}{\sigma_e} \quad (14)$$

The activation overpotentials can be described by the non-linear Butler–Volmer equation, which relates to the current density by considering the charge transfer at the three-phase boundary as a rate-limiting step and the activation overpotentials. The activation overpotentials for the electrochemical reduction of H<sub>2</sub>O and CO<sub>2</sub> are given by

$$i_{H_2} = i_{H_2}^0 \left[ \exp\left(\frac{(1+\beta_a)F\eta_{act,c}}{RT}\right) - \exp\left(-\frac{\beta_c F\eta_{act,c}}{RT}\right) \right] \quad (15)$$

$$i_{CO} = i_{CO}^0 \left[ \exp\left(\frac{\beta_a F\eta_{act,c}}{RT}\right) - \exp\left(-\frac{(1+\beta_c)F\eta_{act,c}}{RT}\right) \right] \quad (16)$$

The Butler–Volmer equation for the anodic activation overpotential can be shown in Eq(17).

$$i_i = i_{O_2}^0 \left[ \exp\left(\frac{\beta_a F\eta_{act,a}}{RT}\right) - \exp\left(-\frac{\beta_c F\eta_{act,a}}{RT}\right) \right] \quad (17)$$

where  $\beta$  is the charge transfer coefficient (usually taken to be 0.5),  $i_1^0$  is the exchange current density. The kinetic and cell parameters can be found in the literatures (Suwanwarangkul, 2003; Janardhanan et al., 2007; Narasimhaiah & Janardhanan, 2013).

### 3. Results and discussion

The SOEC for  $H_2O/CO_2$  co-electrolysis is simulated based on the mathematical equations shown in the previous section. The SOEC model including the mass balances and electrochemical model, which are the nonlinear and differential equations, is solved by using MATLAB. To validate the SOFC model, the I-V characteristic curves of the SOEC from the model prediction is compared with the experimental data performed at DTU Energy conversion (Ebbesen et al., 2012). Table 1 shows cell parameters used for model validation. Figure 2 presents the comparison between the simulated and experimental results. It can be seen that the results of model prediction shows good agreement with the experiment data.

Table 1: Cell parameters for the model validation

Parameters	Value	Parameters	Value
Porosity, $\varepsilon$ (-)	0.35	Cathode thickness, $d_c$ ( $\mu\text{m}$ )	500
Tortuosity, $\xi$ (-)	5.0	Anode thickness, $d_a$ ( $\mu\text{m}$ )	50
Average pore radius, $r_p$ ( $\mu\text{m}$ )	$3.56 \times 10^{11}$	Electrolyte thickness, $d_e$ ( $\mu\text{m}$ )	50

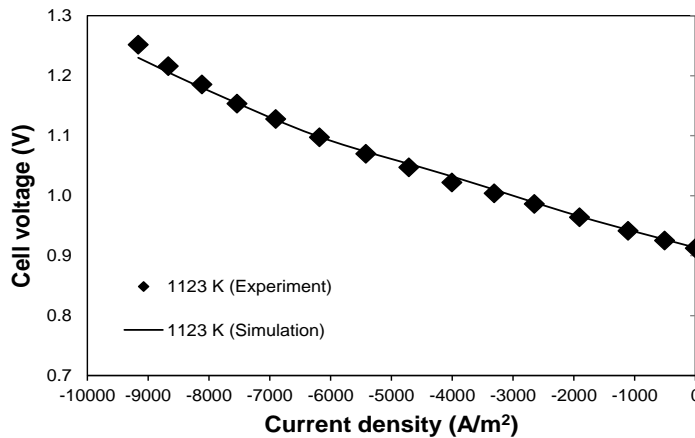


Figure 2: Comparison between the experimental and model-predicted I-V curves of SOEC at 1123 K and 1 bar.

The validated model was used to study the behavior and performance of SOEC. To study the influence of the operating parameters on the SOEC performance for  $H_2O/CO_2$  co-electrolysis, the inlet gas compositions are fixed at 40%  $H_2O$ , 40%  $CO_2$ , 10%  $H_2$ , and 10%  $CO$  and air is introduced at the anode side. To investigate the influence of the RWGS reaction on the cathode for the syngas production from the co-electrolysis in the SOEC, the WGS reaction rate and the gas composition along the cathode thickness at various temperatures are considered in Figure 3a and 3b, respectively. From Figure 3a, it can indicate that the WGS reaction rates are negative value at the cathode surface because of high  $CO_2$  and  $H_2O$  composition. The RWGS reaction has an impact on the cell performance at a range of the cathode thickness between 0-200  $\mu\text{m}$ . Thus, the mole fraction of  $CO$  is higher than that of  $H_2$ , as shown in Figure 3b. The WGS reaction rates increase from the cathode surface to the three-phase boundary along the cathode thickness. This is caused by an increase in the amount of  $CO$ , resulting in a high driving force of the WGSR in the forward direction. When considering the effect of temperature, the WGS reaction rate decreases with increasing temperature at the cathode thickness range of 0-200  $\mu\text{m}$  whereas the increase in temperature enhances the WGS reaction rate at the thicker cathode greater than 200  $\mu\text{m}$ .

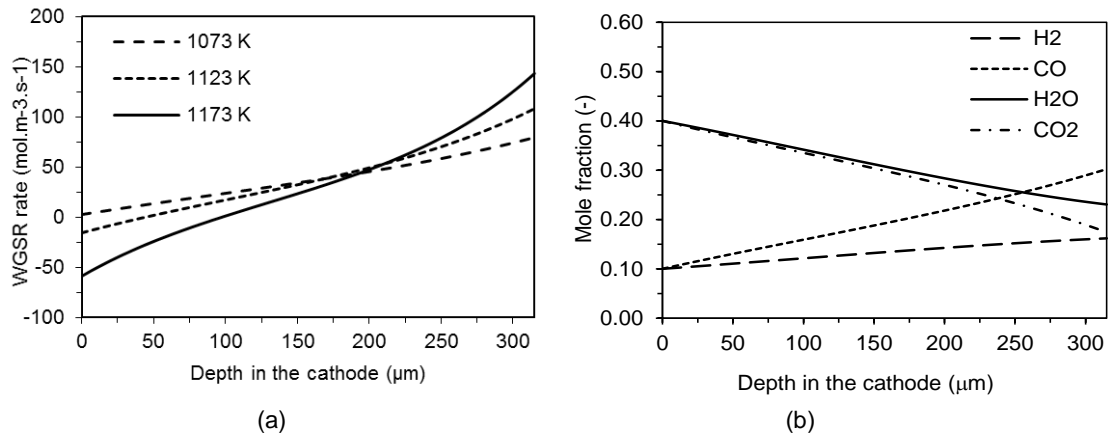


Figure 3: Effect of temperature on (a) WGSR rate and (b) gas composition at 1073 K as a function of the depth in the cathode.

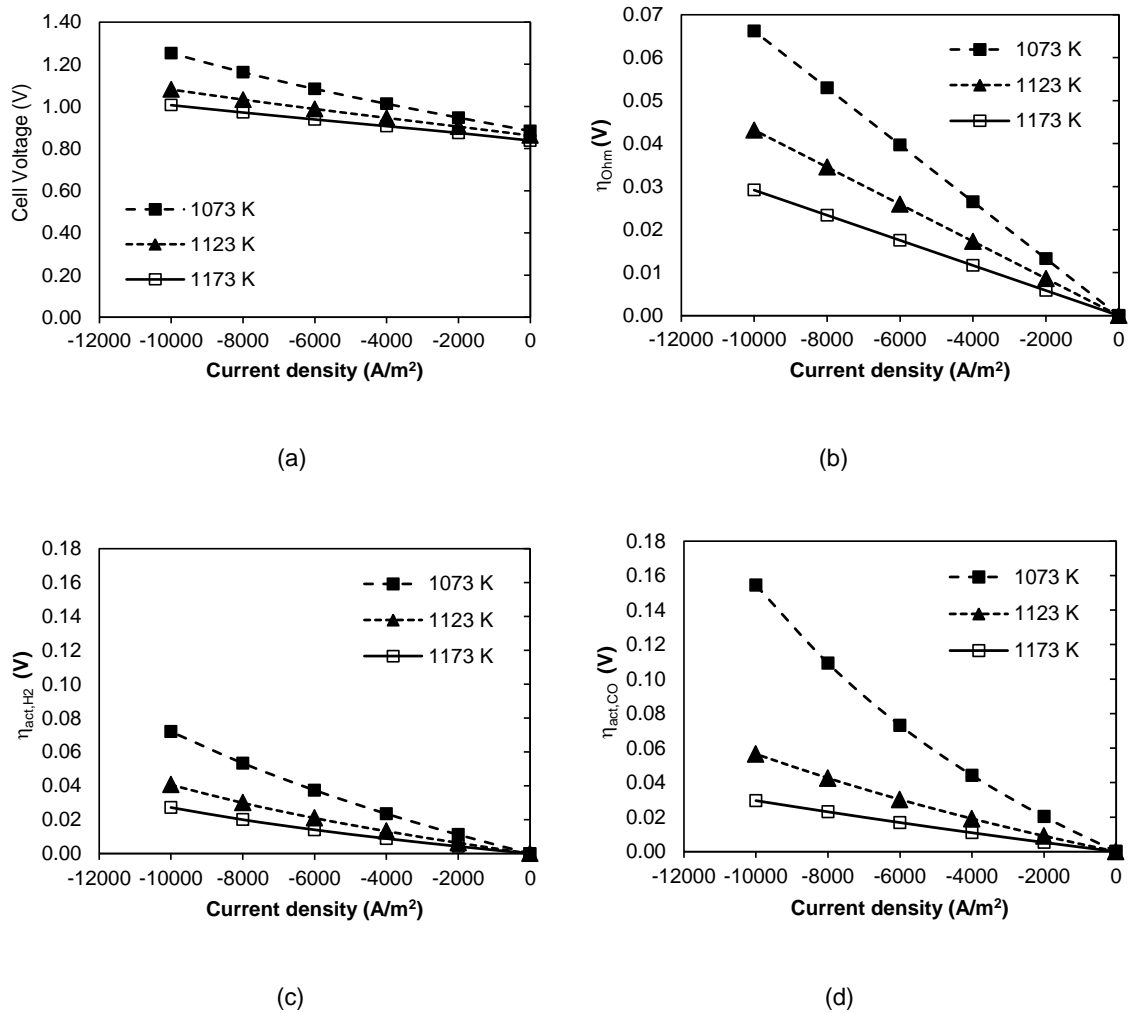


Figure 4: Effect of temperature on (a) cell voltage; (b) ohmic overpotential; (c) activation overpotentials for H<sub>2</sub>O electrolysis; and (d) activation overpotentials for CO<sub>2</sub> electrolysis as a function of current density.

The operating temperature is a key factor affecting the SOEC performance. The effect of operating temperature on the cell voltage as a function of current density for H<sub>2</sub>O/CO<sub>2</sub> co-electrolysis is illustrated in

Figure 4a. It is found that the cell voltage decreases with an increase in the operating temperature, resulting in reduction of the power supply for co-electrolysis in the SOEC. The increase in the operating temperature can increase thermal energy demand. On the contrary, the electrical energy demand subsides and it causes to decrease the reversible voltage.

The effect of the operating temperature on the ohmic overpotentials as a function of the current density is illustrated in Figure 4b. The ohmic overpotentials is lower at higher cell temperature. This is mainly due to the high conductivity of YSZ electrolyte at high operating temperatures, resulting in a decrease in the cell resistance. Moreover, an increase in the operating temperature has an effect on a decrease in the internal voltage losses. Figure 4c and 4d show the activation overpotentials of H<sub>2</sub>O and CO<sub>2</sub> electrolysis as a function of the current density, respectively. It can be seen that the activation overpotentials decrease when the cell temperature increases. This results from the higher rate of the electrode reaction with a higher temperature, leading to the increase in the exchange current density. When comparing the H<sub>2</sub>O and CO<sub>2</sub> electrolysis, the activation overpotentials occurring in the CO<sub>2</sub> electrolysis is higher than that in H<sub>2</sub>O electrolysis about 53.4%, 28.2%, and 7.9% for 1073, 1123 K, and 1173 K, respectively (at the current density of 10,000 A/m<sup>2</sup>). Thus, the increase in operating temperature has high effect on diminishing the activation overpotentials of CO<sub>2</sub> electrolysis.

#### 4. Conclusions

In this study, the electrochemical model of a solid oxide electrolysis cell (SOEC) for H<sub>2</sub>O and CO<sub>2</sub> co-electrolysis is presented and the model prediction is verified by comparing with the experiment data from the literature. The validated model is used to study the effect of a water gas shift (WGS) reaction in the cathode during the H<sub>2</sub>O and CO<sub>2</sub> co-electrolysis on the SOEC performance. It is found that the WGS reaction rate depends on the gas composition and operating temperature. An increase in the operating temperature decreases the WGS reaction rate at the cathode surface, owing to high CO<sub>2</sub> compositions. On the other hand, the CO component is higher at thicker cathode, resulting in an increase in the WGS reaction rate with increasing temperature. Moreover, the power supply required for the co-electrolysis in the SOEC can be reduced by the increase of the operating temperature. The activation and ohmic overpotentials decrease when the cell operates at a higher temperature.

#### Acknowledgements

The authors would like to express their gratitude for financial support from Burapha University (No.152/2559) and the Thailand Research Fund (No. DPG5880003).

#### References

- Ebbesen S.D., Knibbe R., Mogensen M., 2012, Co-Electrolysis of Steam and Carbon Dioxide in Solid Oxide Cells, *Journal of the Electrochemical Society*, 159, F482-F489.
- Ferrero D., Lanzini A., Santarelli M., Leone P., 2013, A comparative assessment on hydrogen production from low- and high-temperature electrolysis, *International Journal of Hydrogen Energy*, 38, 3523-3536.
- Janardhanan V.M., Deutschmann O., 2007, Numerical study of mass and heat transport in solid-oxide fuel cells running on humidified methane, *Chemical Engineering Science*, 62 (18), 5473-5486.
- Kazempoor P., Braun R.J., 2015, Hydrogen and synthetic fuel production using high temperature solid oxide electrolysis cells (SOECs), *International Journal of Hydrogen energy*, 40, 3599-3612.
- Menon V., Janardhanan, V.M., Deutschmann, O., 2014, A mathematical model to analyze solid oxide electrolyzer cells (SOECs) for hydrogen production, *Chemical Engineering Science*, 110, 83–93.
- Narasimhaiah G., Janardhanan V.M., 2013, Modeling CO<sub>2</sub> electrolysis in solid oxide electrolysis cell, *Journal of Solid State Electrochemistry*, 17, 2361-2370.
- Ni M., 2012, 2D thermal modeling of a solid oxide electrolyzer cell (SOEC) for syngas production by H<sub>2</sub>O/CO<sub>2</sub> co-electrolysis, *International Journal of hydrogen energy*, 37, 6389-6399.
- Saebea D., Authayanun S., Patcharavorachot Y., Arpornwichanop A., Enhancement of hydrogen production for steam reforming of biogas in fluidized bed membrane reactor, *Chemical Engineering Transactions*, 39, 1177-1182.
- Saebea D., Authayanun S., Patcharavorachot Y., Arpornwichanop A., Performance evaluation of low-temperature solid oxide fuel cells with SDC-based electrolyte, *Chemical Engineering Transactions*, 52, 223-228.
- Suwanwarangkul R., Croiset E., 2003, Performance comparison of Fick's, dusty-gas and Stefan-Maxwell models to predict the concentration overpotentials of a SOFC anode, *Journal of Power Sources*, 9-18.